

2 Design Tools

**Volker Pickert, Keith Pullen,
Andrew Forsyth, Dave Stone**

**Project Management Meeting
The University of Manchester
Monday 7th April 2014**



Scope of Theme

step 1

Online survey on:

Missing electrical,
thermal and mechanical
links of today's
Simulators
(Newcastle)

Step 2

Specific effects:

- Prediction of convective heat transfer in electric machines
(City)
- Loss mechanism and heat removal in inductors for dc/dc converters
(Manchester)

Step 3

Development of new heat removal techniques:

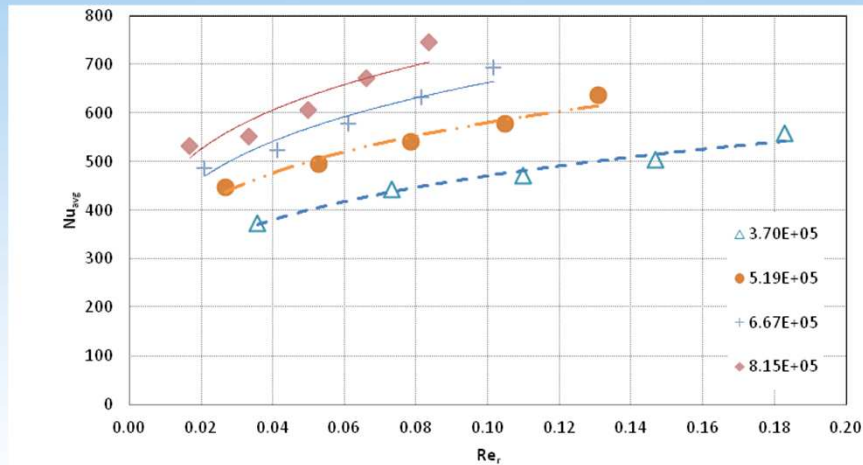
- Liquid cooler with locally changing thermal impedances
(Newcastle)
- High thermal conductivity potting compounds
(Sheffield)



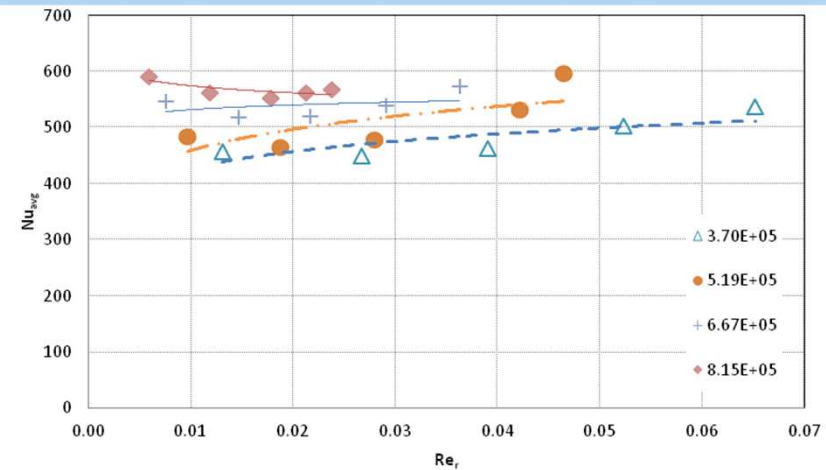


Current results

Correlation of experimental results to Re_r from Bayley (1971) – breaks down at large gap ratio



Average heat transfer against inlet and rotational Reynolds number ratio for forced radial out-flow and gap ratio 0.0106



Average heat transfer against inlet and rotational Reynolds number ratio for forced radial out-flow and gap ratio 0.0297

$$Re_r = \frac{C_w}{2\pi G Re_\omega}$$



CITY UNIVERSITY
LONDON



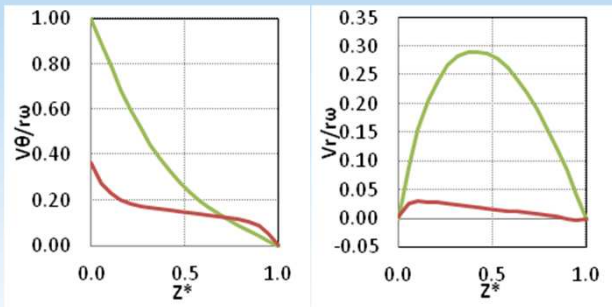
Current results

CFD results – 2D model

Forced flow dominates in laminar regime

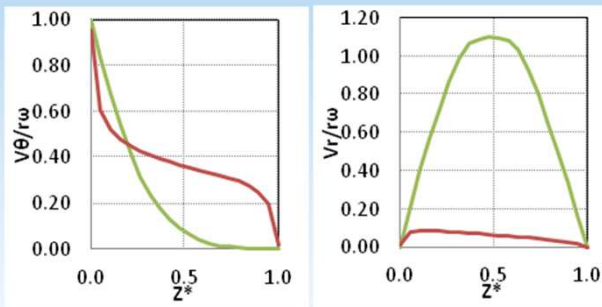
Batchelor flow type (separate boundary layers) in turbulent regime for ALL forced outflow

Ingress of ambient air at periphery causes drop in temperature, more pronounced in laminar regime



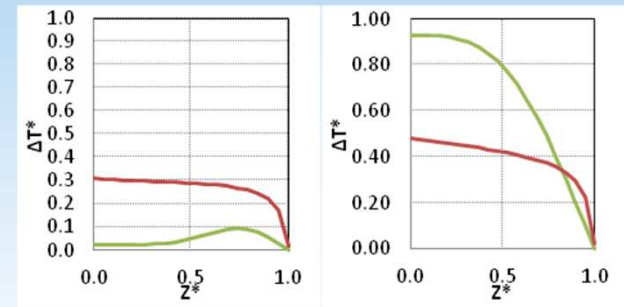
— LAM 200 RPM — SST 2700 RPM

Velocity profiles at $r/R = 0.99$, $G = 0.0106$ and $C_w = 9e2$ for forced radial out-flow



— LAM 200 RPM — SST 2700 RPM

Velocity profiles at $r/R = 0.99$, $G = 0.0106$ and $C_w = 3.6e3$ for forced radial out-flow



— LAM 200 RPM — SST 2700 RPM

Comparison of temperature profiles, $r/R = 0.99$, $G = 0.0106$, left: no forced flow, right: $C_w = 3.6e3$ forced radial out-flow



CITY UNIVERSITY
LONDON

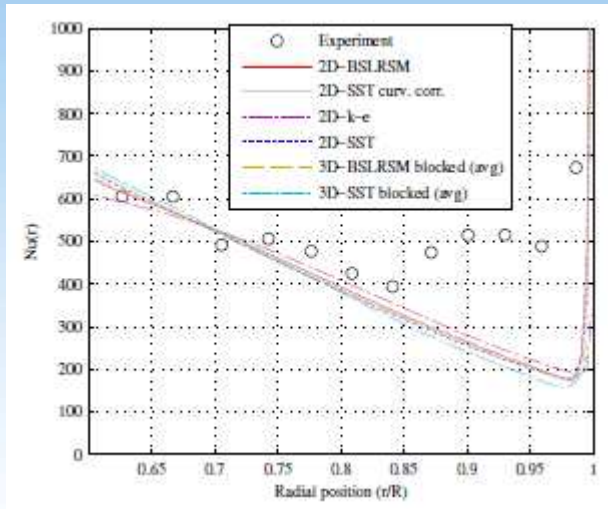


Current results

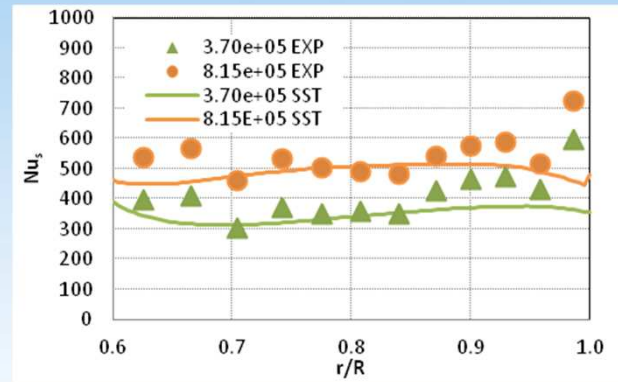
Comparison of CFD to experimental results

Forced outflow is better predicted by CFD - however - under prediction at the periphery still apparent and CFD model needs to be adapted

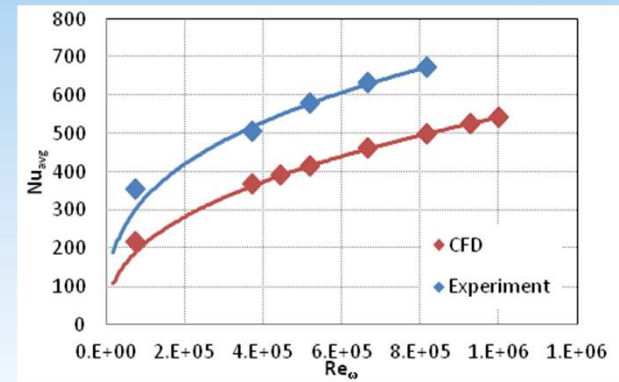
Result is general under-prediction of average heat transfer results



Comparison of CFD calculation and experimental measurement of radially resolved heat transfer against rotational speed for $G = 0.0106$ with no forced throughflow from Howey (2011)



Comparison of CFD calculation and experimental measurement of radially resolved heat transfer against rotational speed for $G = 0.0106$, $C_w = 3.6e2$ radial out-flow



Comparison of CFD calculation and experimental measurement of average heat transfer against rotational speed for $G = 0.0106$, $C_w = 3.6e2$ radial out-flow, turbulent correlations projected backward.

Progress and future work plan

Rotor Stator Disc System with no superposed (net) flow

Geometric properties	
Input parameters	Units
s	0,05 m

Please choose in the list the kind of regime			
regime 1: laminar flow, small gap, merged BL	regime 2: laminar flow, large gap, separate BL	regime 3: turbulent flow, small gap, merged BL	regime 4: turbulent flow, large gap, separate BL

Summary: **Single Disc (Free Rotor)** **Rotor disc with**

Windage Loss		
Windage Loss (power)	3,07876E+19	(W)
Torque	3,07876E+15	(Nm)
Torque coefficient	6,91856E-05	regime 1: laminar flow, small gap, merged BL
	false	regime 2: laminar flow, large gap, separate BL
	false	regime 3: turbulent flow, small gap, merged BL
	false	regime 4: turbulent flow, large gap, separate BL
	false	5x105 < Reω < 2x106 0.0125 ≤ G ≤ 0.1
Rotational Reynolds number	90816326,53	
G	0,0005	

Determination of the loss, flow and heat transfer in the radial and axial gaps of rotating cylinders and discs

sheet 1	Single Disc (Free Rotor)
sheet 2	Rotor Stator Disc System with no superposed (net) flow
sheet 3	Rotor Stator system with superposed (net) radial flow
sheet 4	Rotating Cylinder in an Annulus
sheet 5	Rotating cylinder in annulus with superposed axial flow

Each sheet is specialized for one case.

input the values that are shared for all the cases, and then go to the sheet specialized for the case you need.

Values that are shared for all the cases		
Geometric properties		
Input parameters		Units
ω	10000	rad/s
R=a	100	m
Gas properties		
Input parameters		Units
k	85	
ρ	85	kg/m³
μ	38	Pa.s

Discs

Cylinders

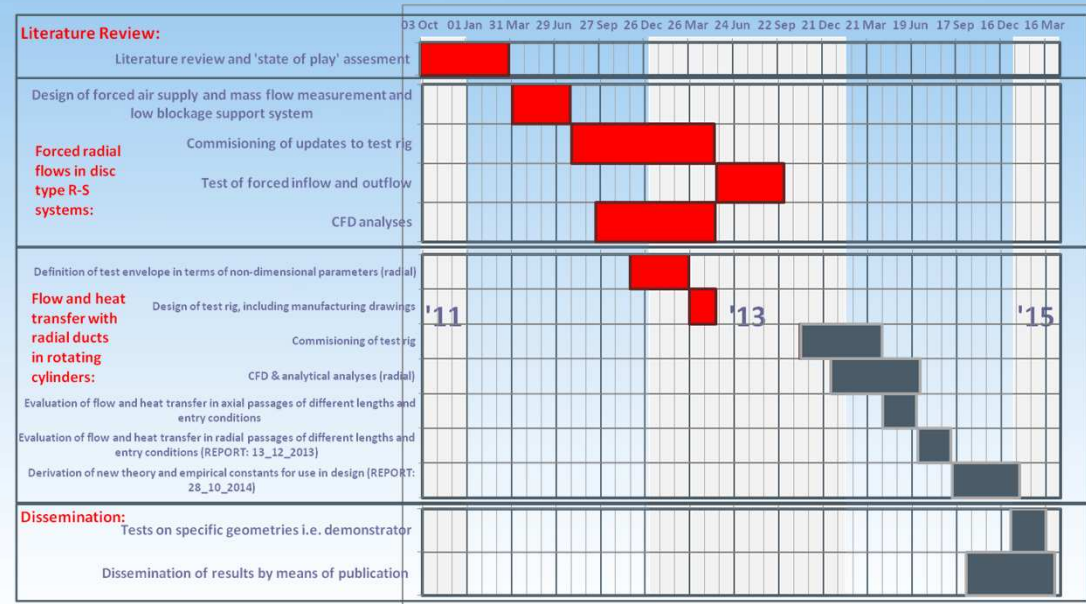
- Transfer report completed
- Paper submitted to ICEM XXI International Conference on Electrical Machines 2014, Berlin, Germany
- Beginnings of a design tool that will bring together all correlations found in order to predict windage, pressure drops and heat transfer in electric machines



Progress and future work plan

Planned future work

- 3D CFD model and improvements
- Paper disseminating 3D results
- Drum-type test rig commissioned
- CFD analysis for drum type model
- Experiments on drum-type rig
- Paper disseminating drum-type rig results
- Final output of design tool for windage, pressure drops and heat transfer
- Final PhD report



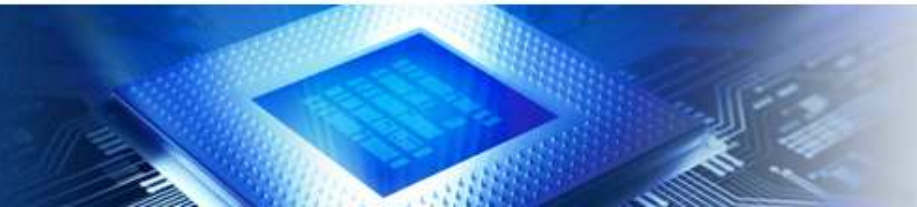
CITY UNIVERSITY
LONDON





The
University
Of
Sheffield.

ves



Introduction

- Reasons for using encapsulants:
 - Enhance mechanical integrity of component
 - Seal component against environment
 - **Improve thermal performance of component by displacing trapped air within component**
- This can be further enhanced by combining the encapsulant with a thermally conductive filler

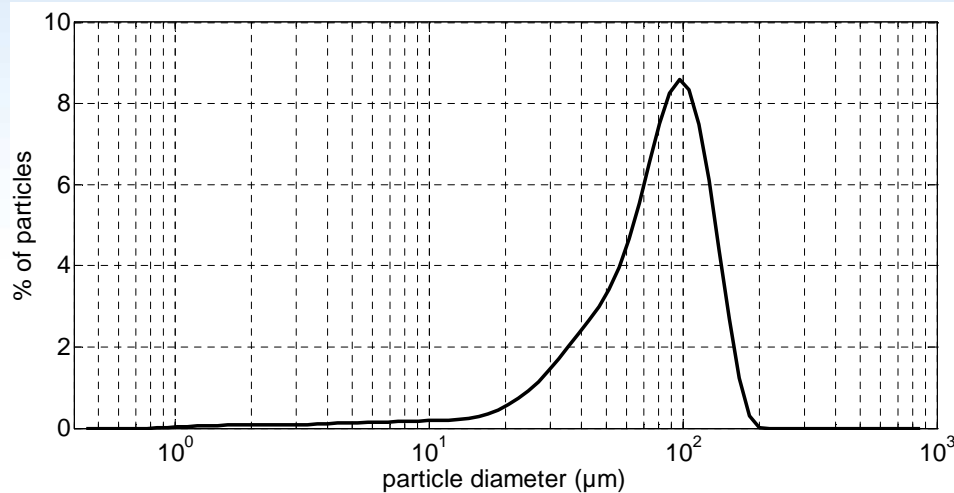


The
University
Of
Sheffield.

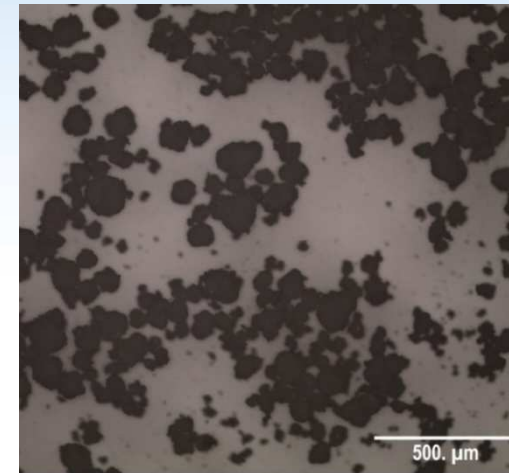


Filler Properties

- The filler used in this work is aluminium oxide powder
 - Theoretical density = 3.97 g/cm^3
 - Thermal conductivity 30 W/m.K
- Poured Density = 0.84 g/cm^3 (21.2% of theoretical density)
- Tapped Density = 1.11 g/cm^3 (28.0% of theoretical density)
- Particles are approximately spherical



Particle size distribution of powder



Microscope image of powder

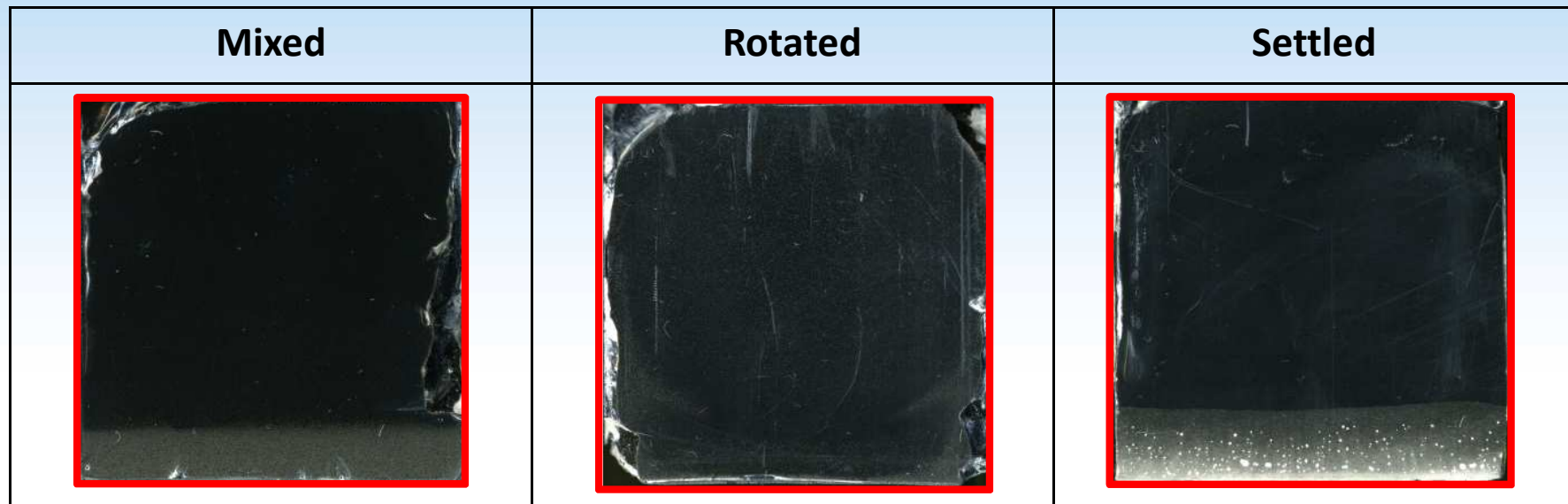


The
University
Of
Sheffield.



Sample production methods

- Different methods were used to produce the samples to allow differences in filler distribution to be considered



Blocks with a 5% filler concentration (by volume) produced using each method



Sample production methods

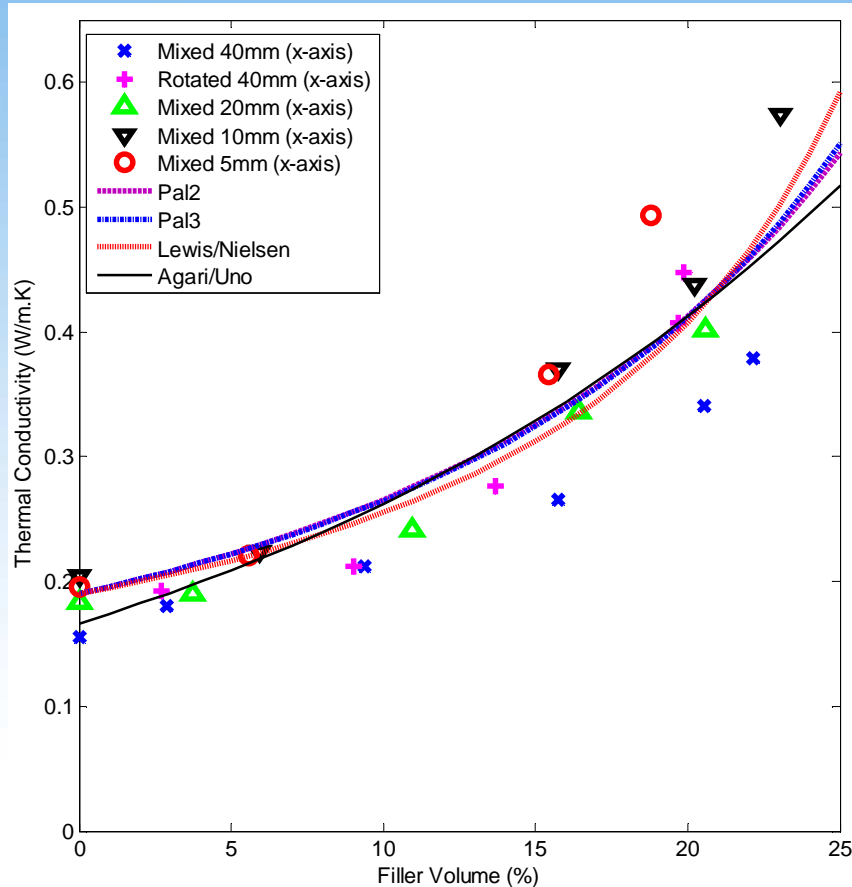
- Mixed samples were produced to examine how the filler is distributed under normal conditions
- Rotated samples were produced in a manner which inhibits the settling of the filler particles
- Settled samples were produced to have a particularly uneven filler distribution (more so than the mixed samples)



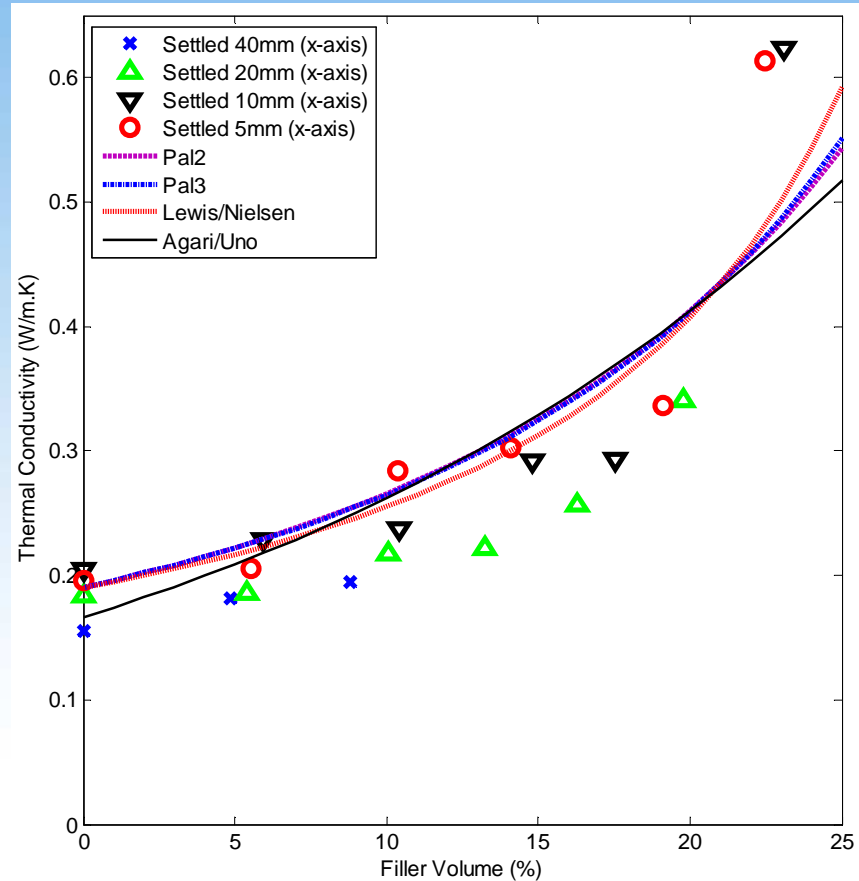
The
University
Of
Sheffield.



Results – Empirical models



Mixed and Rotated block thermal conductivities (shown with empirical models)



Settled block thermal conductivities (shown with empirical models)

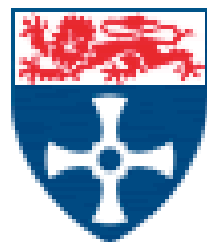


Conclusions

- Dataset can be divided into three groups

Dilute (0% - 10%)	Intermediate (10% - 20%)	Full (20% +)
<ul style="list-style-type: none">▪ Low filler loading level leads to only a small change in thermal conductivity▪ Filler distribution not important	<ul style="list-style-type: none">▪ Manufacturing technique influences filler distribution▪ Effects of this can not be ignored when modelling composites▪ More homogeneous samples exhibit higher bulk thermal conductivity	<ul style="list-style-type: none">▪ Samples can be considered homogeneous as a full fill occurs regardless of manufacturing technique



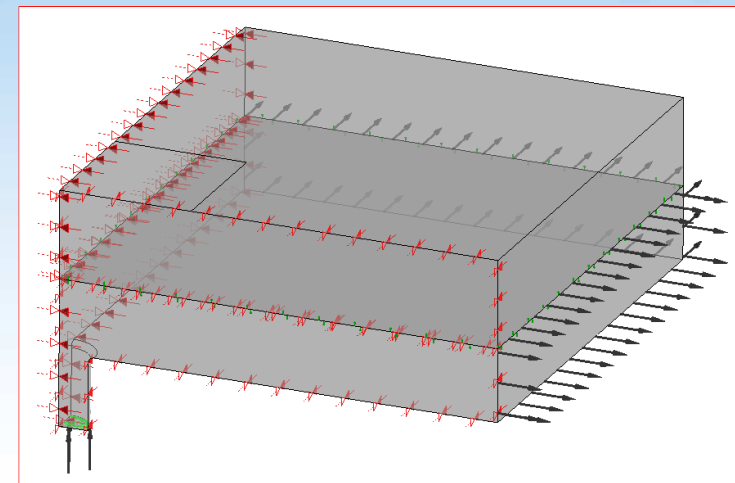
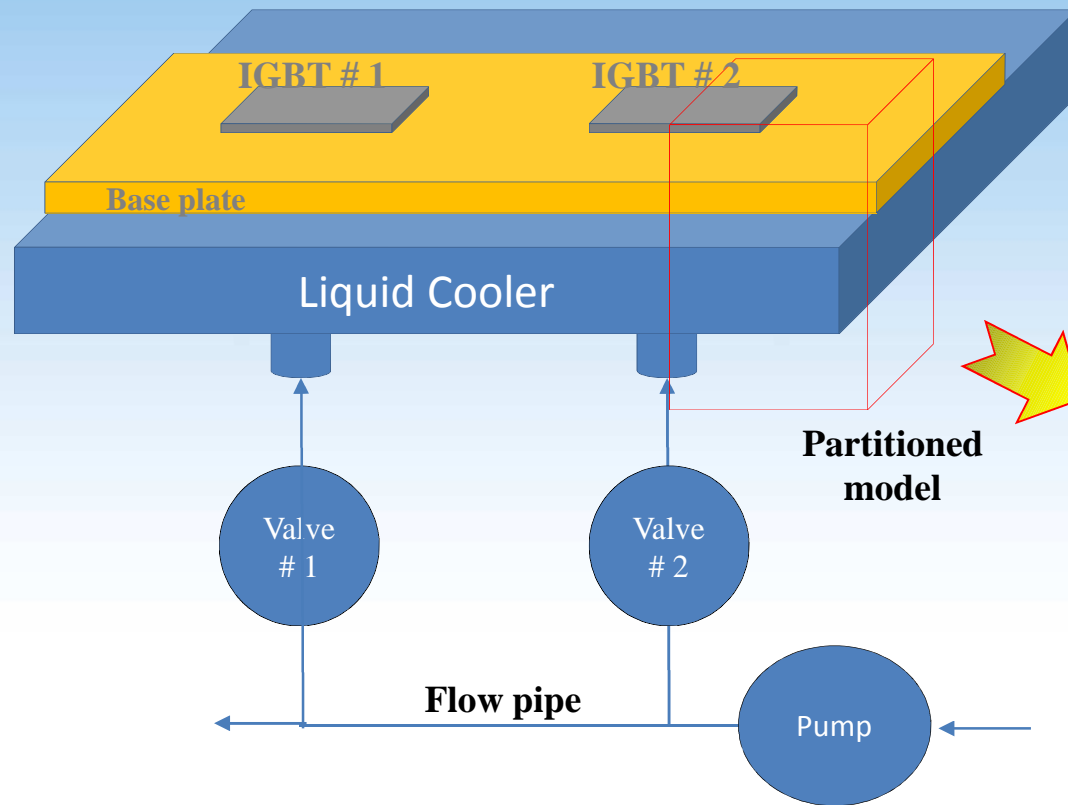


Newcastle
University

ves



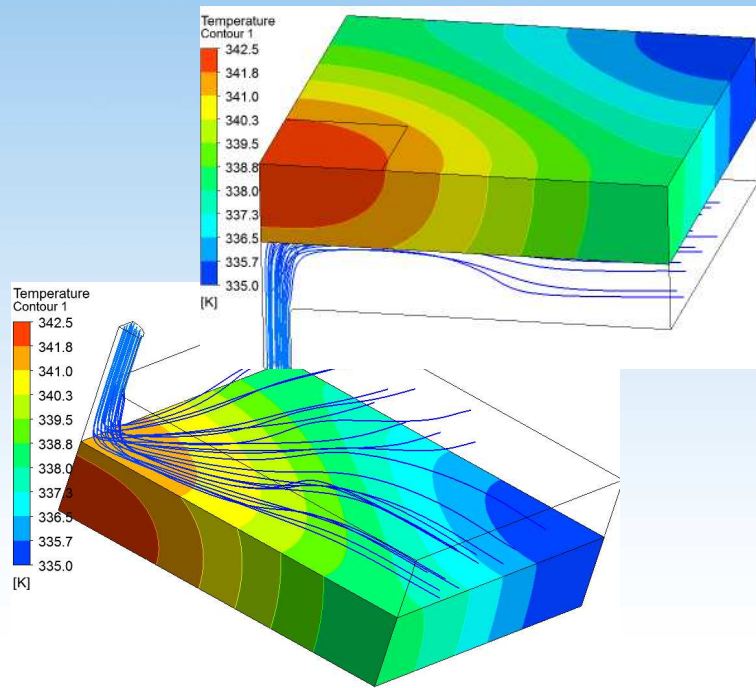
Cooling System Model



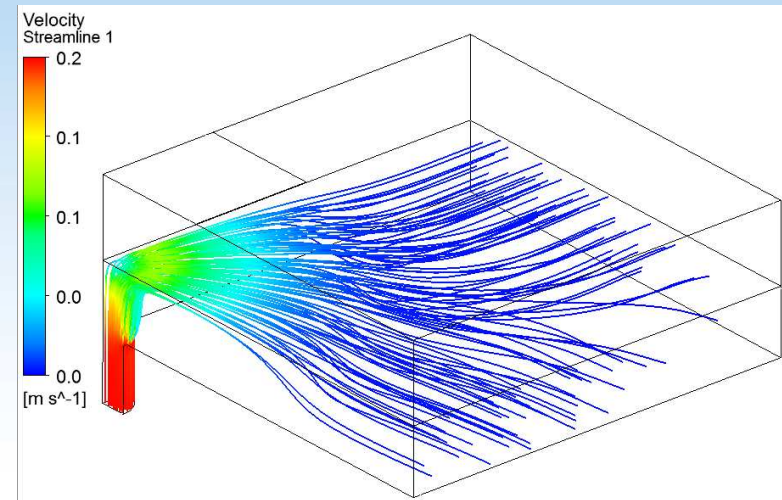
CFD model (ANSYS CFX 14.5)



CFD Analysis of the Liquid Cooler



Temperature

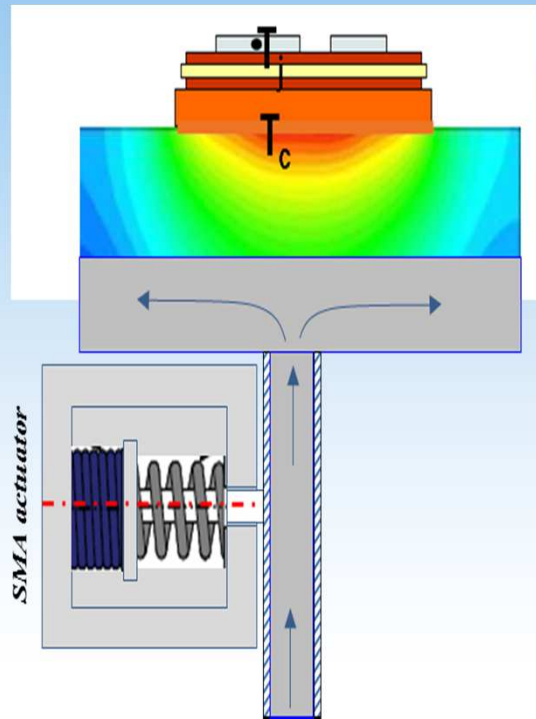


Liquid velocity

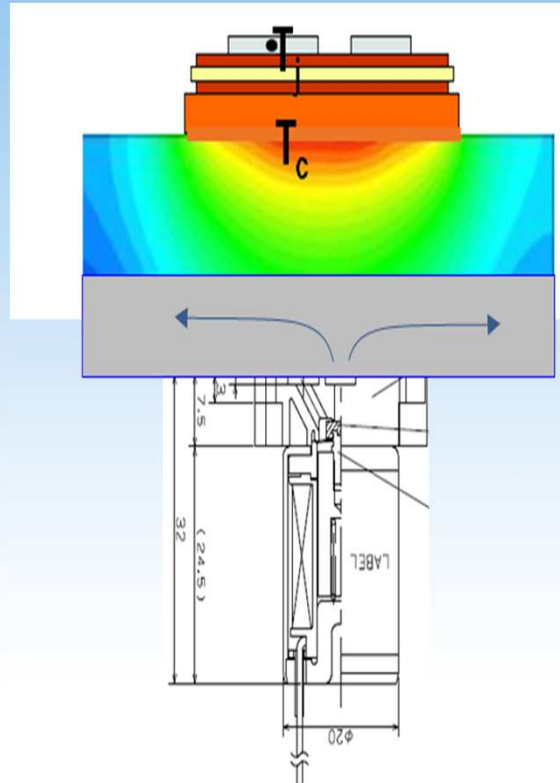
CFD results



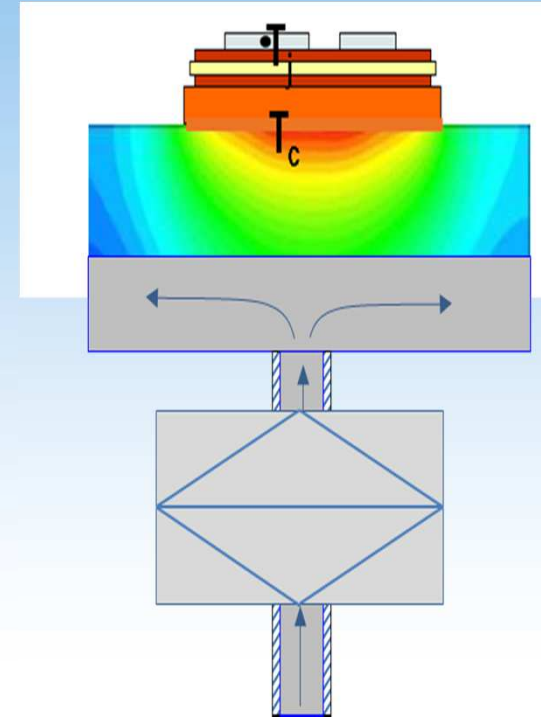
Comparison of valve techniques



SMA spring
(SAES Group, Italy)



Solenoid valve
(Orion Valves Ltd, Japan)

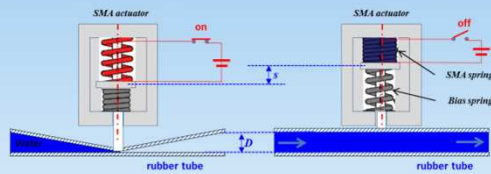


Micro-valve
(Kemikro, Germany)



Dimensions

20 × 20 × 25mm³



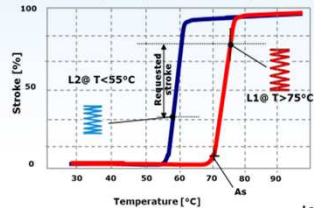
Note:
1. $s = D = 5\text{mm}$;
2. $P_{\text{water}} < 5000\text{Pa}$;
3. $f_{\text{actuator}} = 0.5\text{Hz}$;

Designed by NCL

SMA Spring – Preliminary design

SMA Spring heated by Joule effect expands generating the actuation force for the release of the pin lock. A typical hysteresis cycle for the SMA spring (fig. 1 below) shows how shape memory alloy starts the typical transformation over the A_s (austenite Temperature)

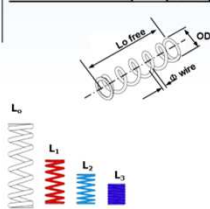
Expected Hysteresis @ constant Load (i.e. F = 10N)



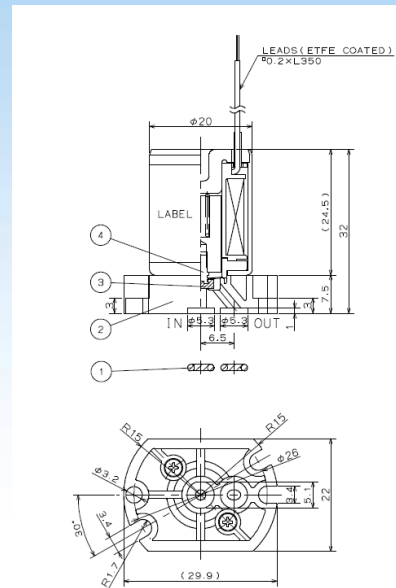
L_0 @ RT no external force
 $L_1 = 20\text{ mm}$ @ $T > 75^\circ\text{C}$
 $L_2 = 15\text{ mm}$ @ $T < 50^\circ\text{C}$
 $L_3 \sim 12\text{ mm}$ block length @ RT

SMA Spring preliminary design

SMA Spring Details	
ϕ spring wire	1 [mm]
OD	10 [mm]
ID	5 [mm]
L spring free	L_0 ~25 [mm]
N° total coils	12
N° active coils	10
Stroke	>5 [mm]

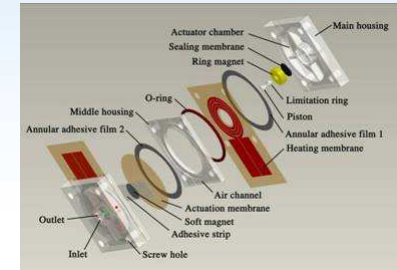
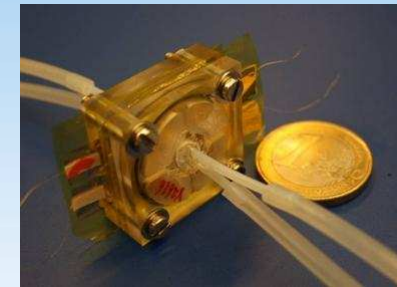


22 × 30 × 32mm³



Solenoid valve
(Orion Valves Ltd, Japan)

26 × 26 × 11mm³

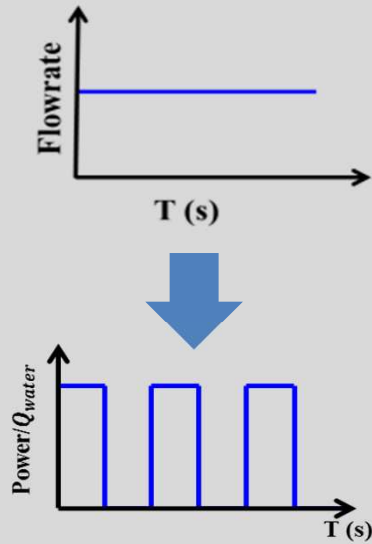


Micro-valve
(Kemikro, Germany)

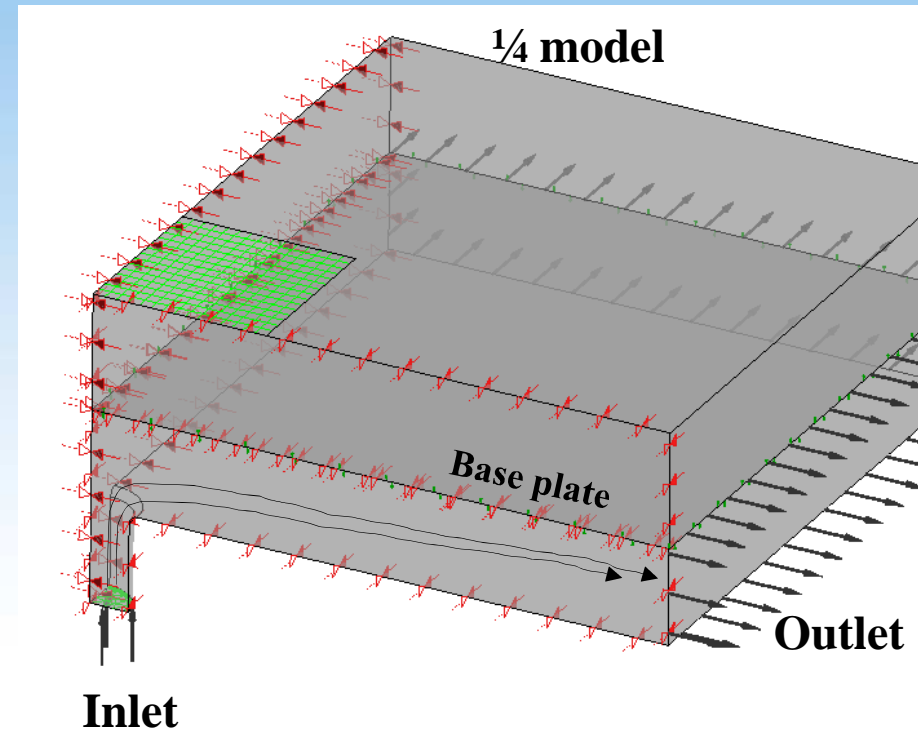
ves



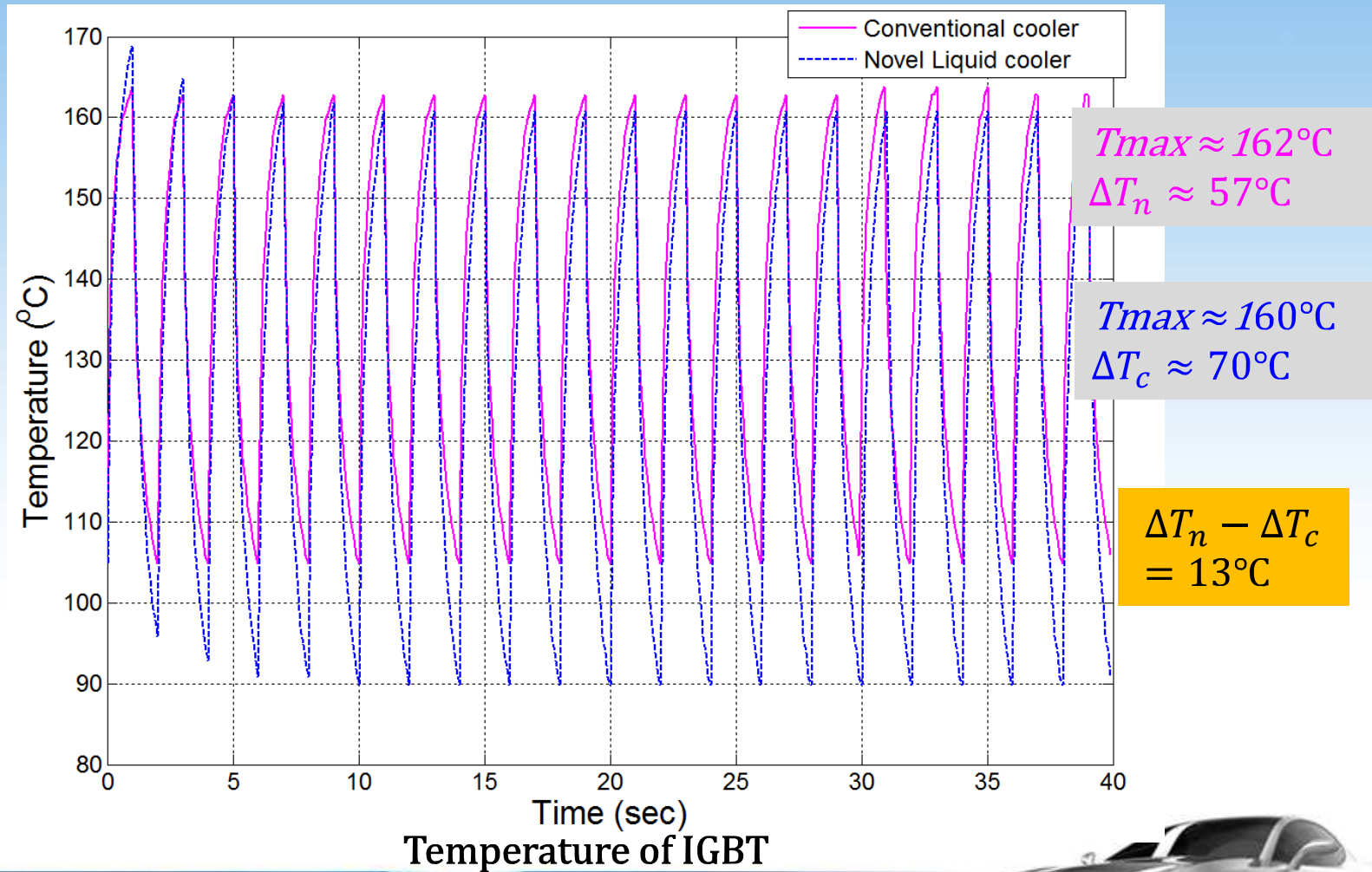
Benefit of using the flow rate actively



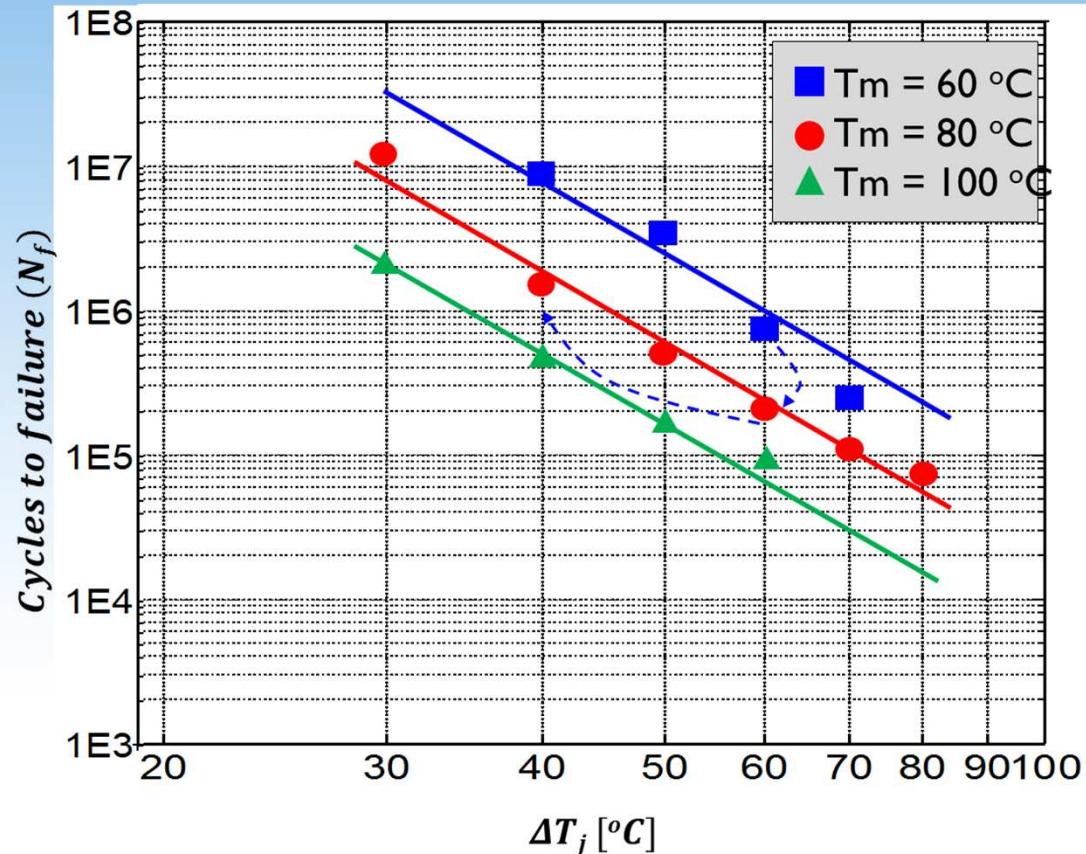
Dissimilar to conventional constant flow rate, a periodic flow rate is calculated based on the pressure vs flow rate curve of the system (pump pressure, pipe diameter and valve speed) .



CFD simulation results



1. CFD Analysis of the Liquid Cooler



$$\Delta T_n - \Delta T_c = 13^\circ\text{C}$$

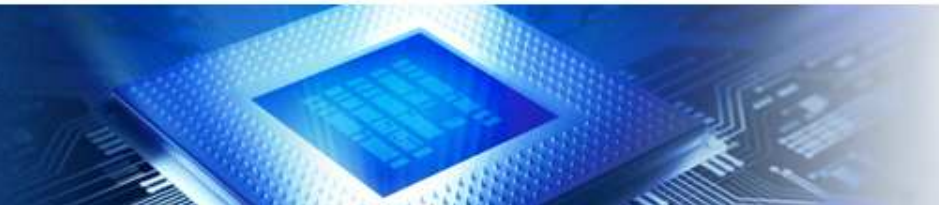
The lifetime of the IGBT module cooled by the new liquid cooler increases approximately by the factor of two compared to a conventional cooler.

Held, M., et al. "Fast power cycling test of IGBT modules in traction application." 1997 International Conference on. Vol. 1. IEEE, 1997.
 Auerbach, F., and A. Lenniger. "Power-cycling-stability of IGBT-modules." Thirty-Second IAS Annual Meeting, IAS'97., Vol. 2. IEEE, 1997.

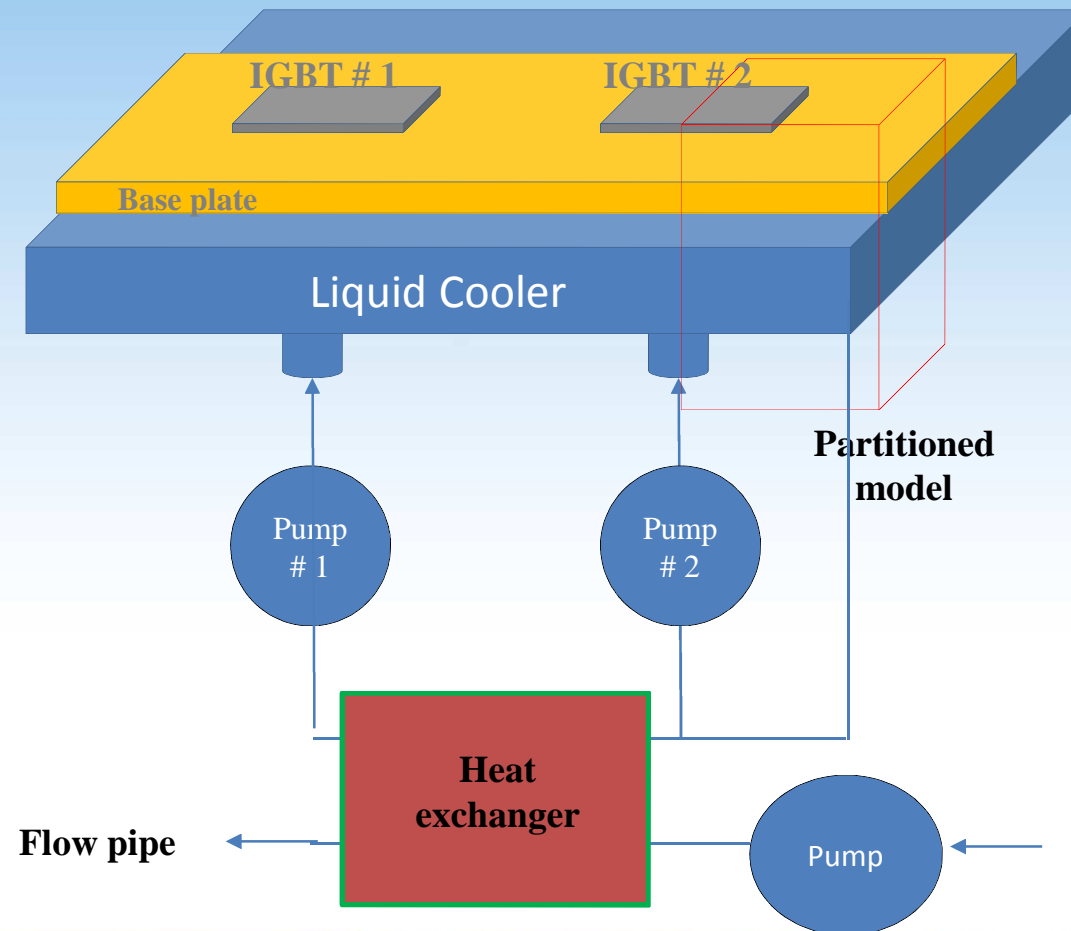


Lifetime of power modules increases but:

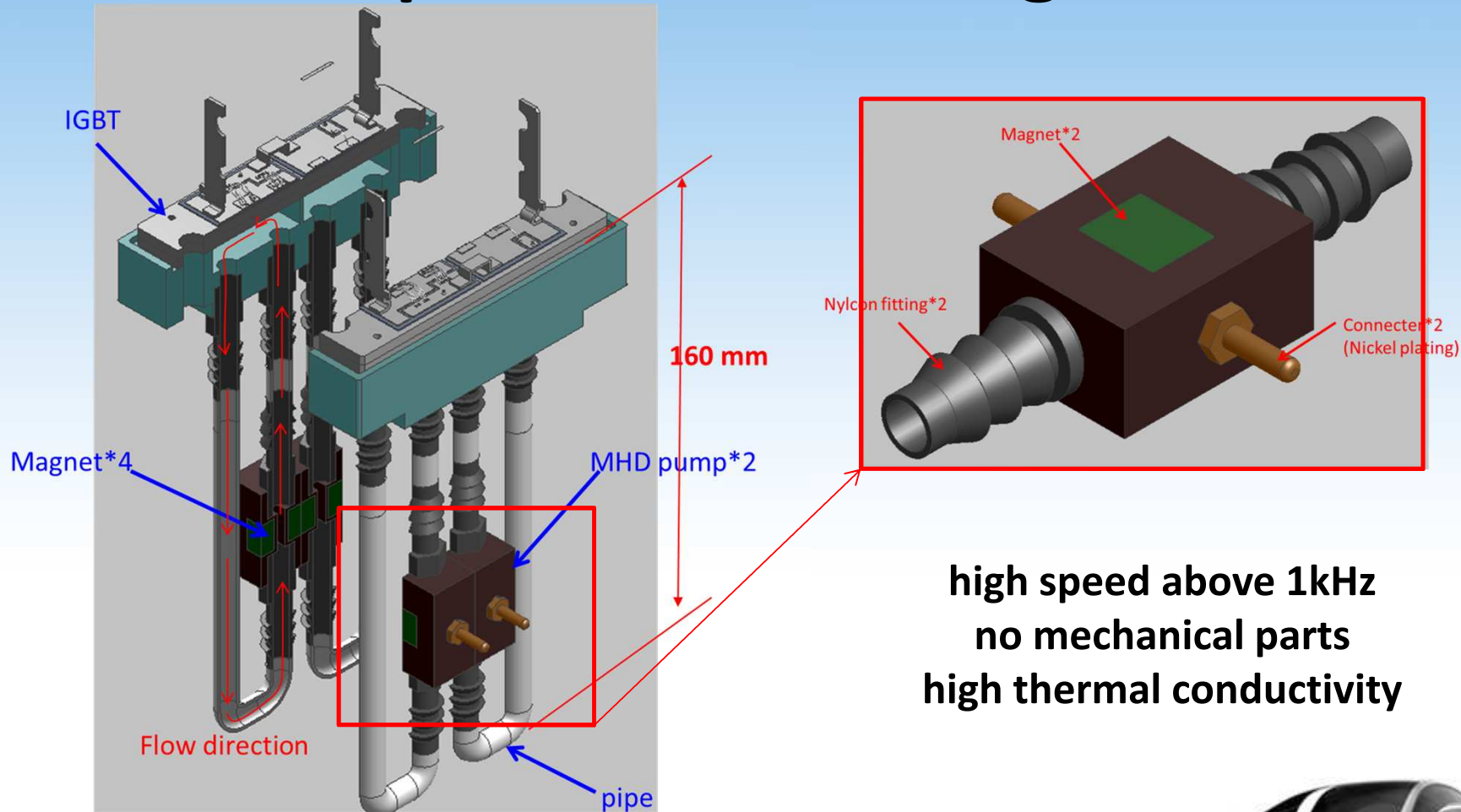
- Lifetime is now dependent on the reliability of the valves. It is predicted that the lifetime is low due to embedded mechanical parts.
- The frequency of the valves is low. Although the Orion valve can work up to 1kHz a faster operating valve would be preferable.
- The size of all valves are still too large.



New approach: use pumps rather valves



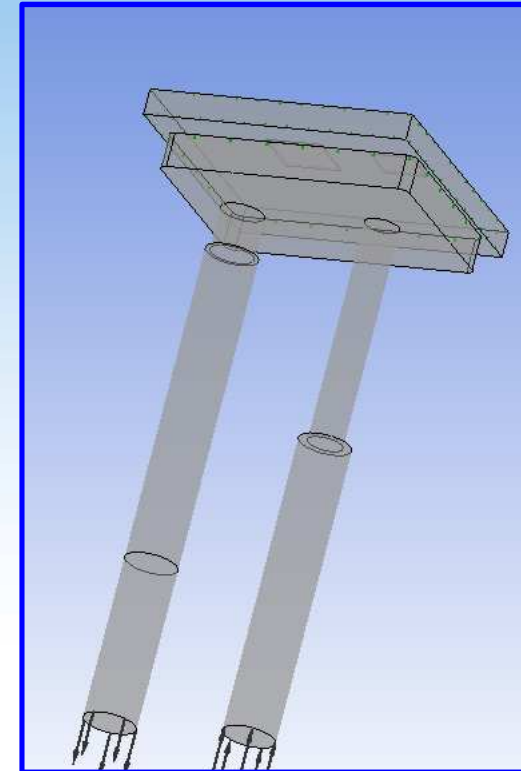
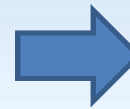
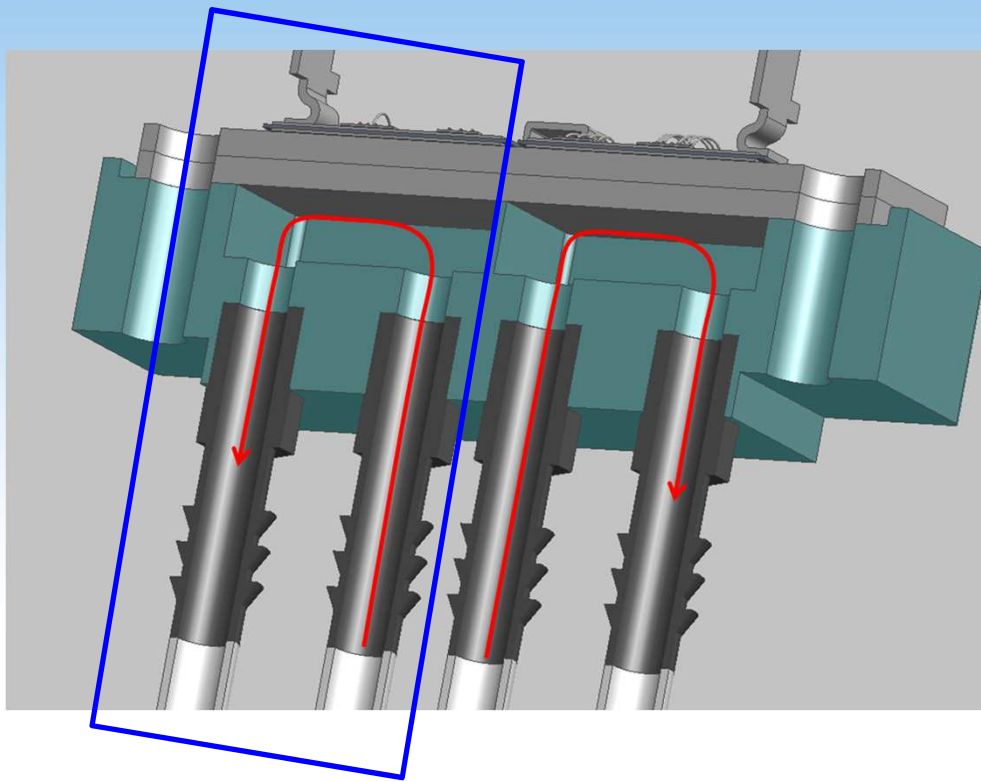
Magneto Hydro Dynamic (MHD) Pump with liquid metal cooling medium



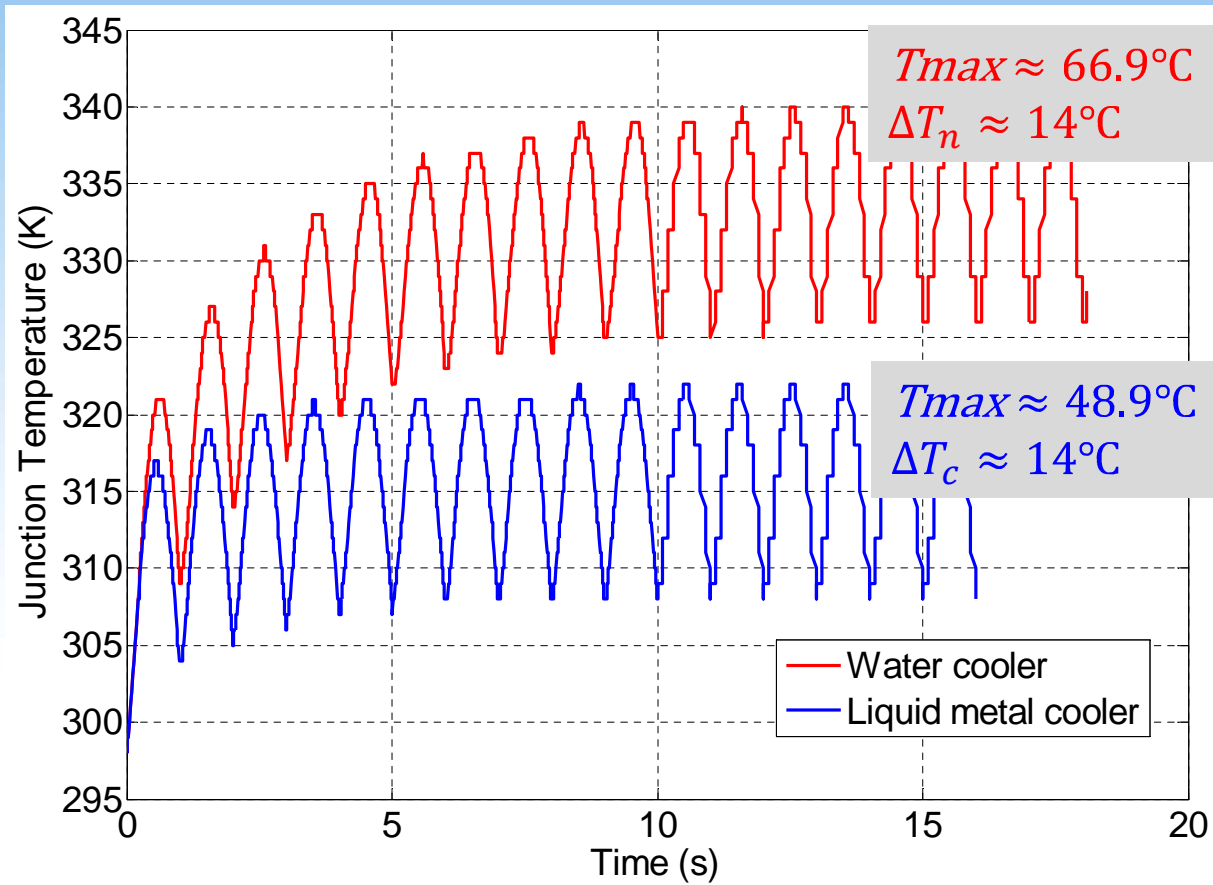
high speed above 1kHz
no mechanical parts
high thermal conductivity



Physical layout

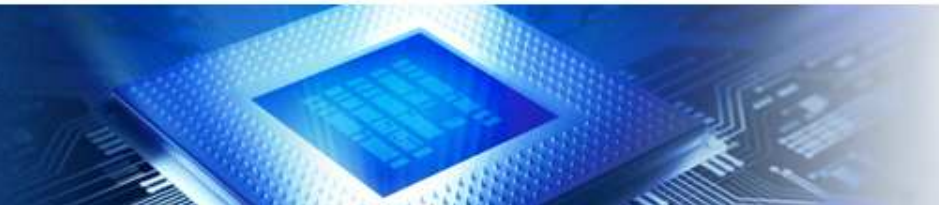


Liquid metal vs. water



Conclusion

1. Liquid metal cooler has better thermal performance than water;
2. Liquid metal cooler has simpler structure than the proposed coolers with micro-valves;
3. MHD pump is more reliable and quieter compared to micro-valves have no moving components;
4. MHD pump is easy to control as the power is proportion to the given control current;
5. MHD pump can operate above 1kHz.



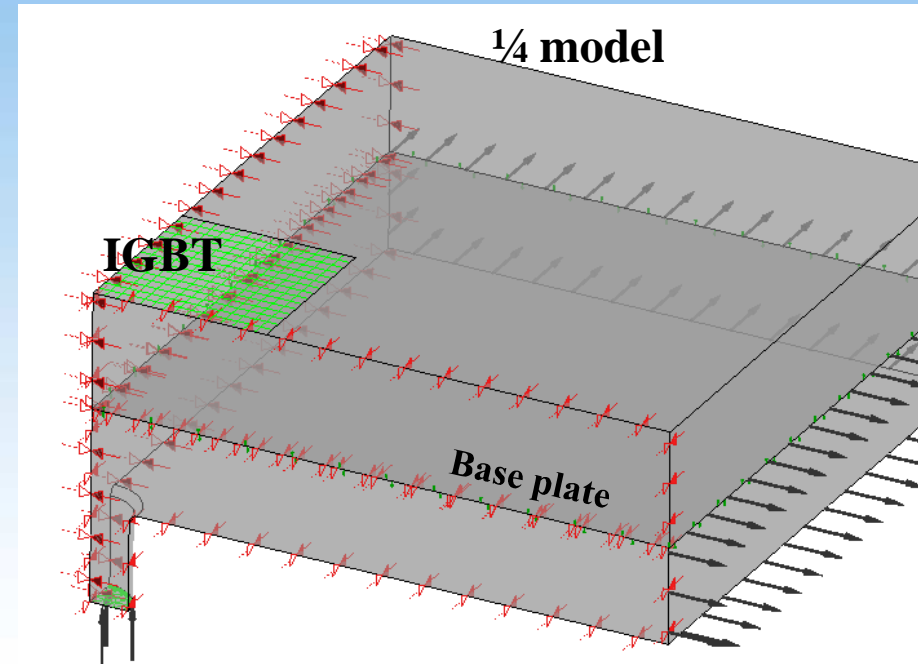
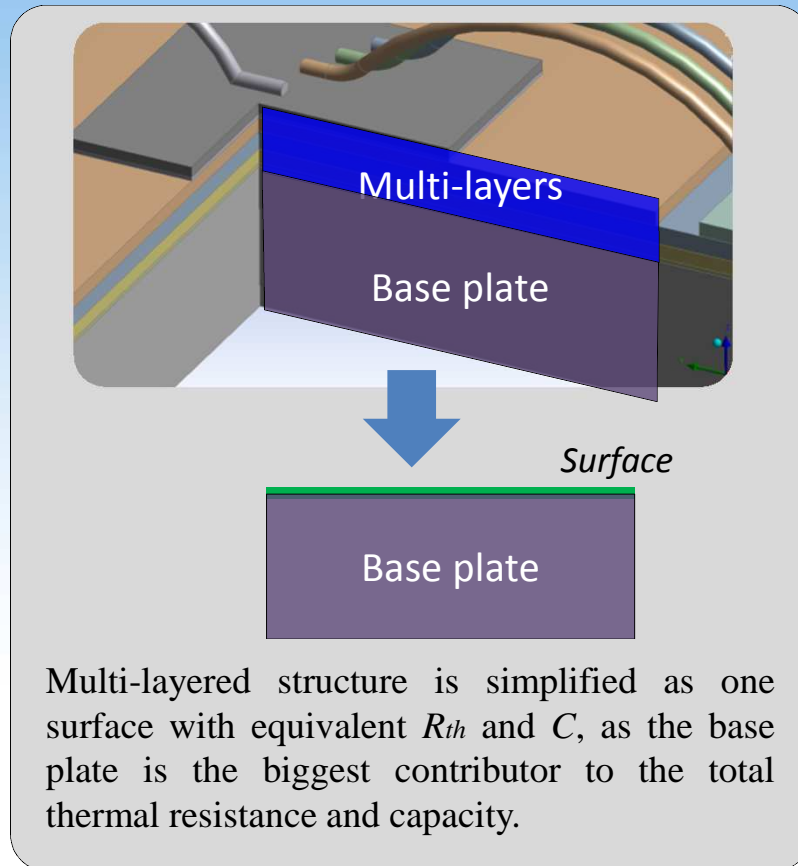
Next Steps

1. Simulation results at high frequency must be further investigated;
2. Construction is on its way.





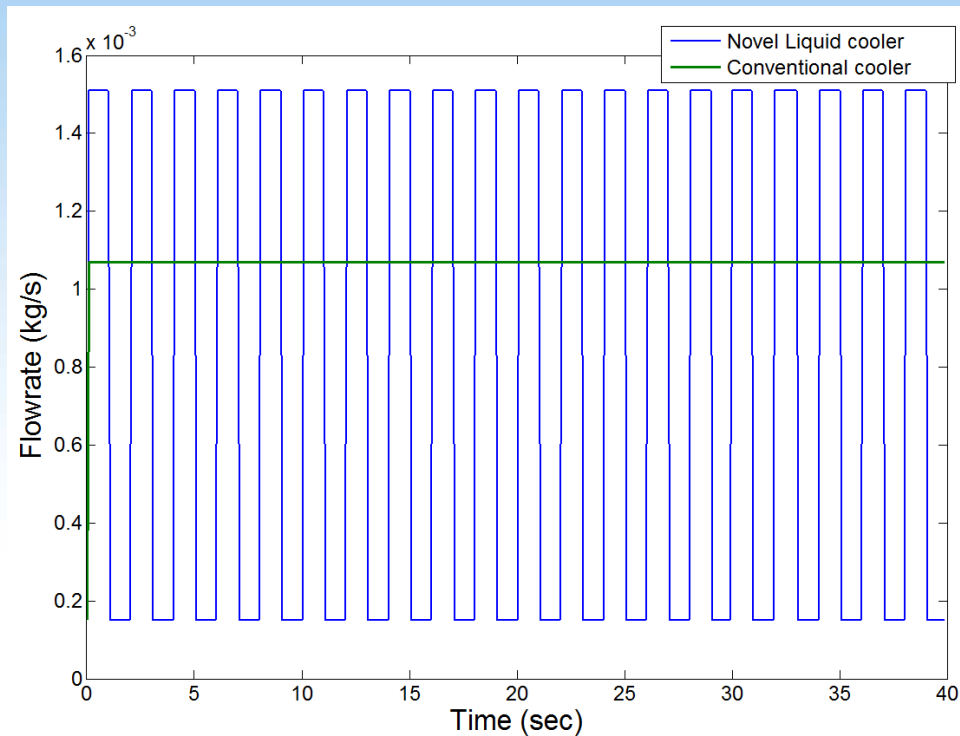
1. CFD Analysis of the Liquid Cooler



Simplification of the multi-layered IGBT structure



1. CFD Analysis of the Liquid Cooler



Initial condition of the simulation:

1. On/off frequency of IGBT: 0.5
2. Flowrate of the conventional cooler is set as $Q = 1.07E3 \text{ Kg/s}$.
3. The max. flowrate of the liquid cooler is set as $\sqrt{2}Q = 1.51E3 \text{ Kg/s}$, which is conservative value (usually among $[\sqrt{2}Q, 2Q]$) based on the flow characteristics of the pump, valve and flow channels.

